Life Sciences 239 (2019) 116878

Contents lists available at ScienceDirect

Life Sciences

journal homepage: www.elsevier.com/locate/lifescie

Deferiprone and efonidipine mitigated iron-overload induced neurotoxicity in wild-type and thalassemic mice

Jirapas Sripetchwandee[a,b], Juthamas Khamseekaew[b], Saovaros Svasti[c], Somdet Srichairatanakool[d], Suthat Fucharoen[c], Nipon Chattipakorn[a,b], Siriporn C. Chattipakorn[a,b,e,*]

[a] Neurophysiology Unit, Cardiac Electrophysiology Research and Training Center, Faculty of Medicine, Chiang Mai University, Chiang Mai, 50200, Thailand
[b] Department of Physiology, Faculty of Medicine, Chiang Mai University, Chiang Mai, 50200, Thailand
[c] Thalassemia Research Center, Institute of Molecular Biosciences, Mahidol University, Nakhon Pathom, 73170, Thailand
[d] Department of Biochemistry, Faculty of Medicine, Chiang Mai University, 50200, Thailand
[e] Department of Oral Biology and Diagnostic Sciences, Faculty of Dentistry, Chiang Mai University, Chiang Mai, 50200, Thailand

ARTICLE INFO

Keywords:
Iron-overload
Oxidative stress
Iron chelator
T-type calcium channel blockers
Mitochondria

ABSTRACT

Aims: We previously demonstrated that iron-overload in non-thalassemic rats induced neurotoxicity and cognitive decline. However, the effect of iron-overload on the brain of thalassemic condition has never been investigated. An iron chelator (deferiprone) provides neuroprotective effects against metal toxicity. Furthermore, a T-type calcium channels blocker (efonidipine) effectively attenuates cardiac dysfunction in thalassemic mice with iron-overload. However, the effects of both drugs on brain of iron-overload thalassemia has not been determined. We hypothesize that iron-overload induces neurotoxicity in Thalassemic and wild-type mice, and not only deferiprone, but also efonidipine, provides neuroprotection against iron-overload condition.

Main methods: Mice from both wild-type (WT) and β-thalassemic type (HT) groups were assigned to be fed with a standard-diet or high-iron diet containing 0.2% ferrocene/kg of diet (HFe) for 4 months consecutively. After three months of HFe, 75-mg/kg/d deferiprone or 4-mg/kg/d efonidipine were administered to the HFe-fed WT and HT mice for 1 month.

Key findings: HFe consumption caused an equal impact on circulating iron-overload, oxidative stress, and inflammation in WT and HT mice. Brain iron-overload and iron-mediated neurotoxicity, such as oxidative stress, inflammation, glial activation, mitochondrial dysfunction, and Alzheimer's like pathologies, were observed to an equal degree in HFe fed WT and HT mice. These pathological conditions were mitigated by both deferiprone and efonidipine.

Significance: These findings indicate that iron-overload itself caused neurotoxicity, and T-type calcium channels may play a role in this condition.

1. Introduction

Most thalassemic patients require blood transfusion because of ineffective erythropoiesis-mediated severe anemia. However, blood transfusion results to develop iron-overload condition in those patients. Several studies reported neurocognitive dysfunction in thalassemia patients [1–3]. Those studies demonstrated that β-thalassemic patients developed iron-overload condition with neurological complications as well as neuropsychological impairment [1,3]. These findings indicate that brain dysfunction in thalassemic subjects can be arisen. Therefore, the underlying mechanisms regarding these dysfunctions need to be further investigated.

Brain iron accumulation may be due to a dysregulation in the physiological production of iron transporters [4]. Previous studies showed changes in brain iron-regulatory proteins, particularly in divalent-metal transporter-1 which is observed during pathological conditions such as aging, neurodegeneration, and iron deficiency [5,6]. However, the expression of this regulatory protein under thalassemia with iron-overload has not known.

Interestingly, our previous studies showed that iron-overload rats developed iron-mediated brain pathologies, hippocampal dysplasticity, reduction of dendritic spine number, and Alzheimer's like pathologies, which subsequently led to cognitive impairment [7,8]. However, brain

* Corresponding author. Neurophysiology Unit, Cardiac Electrophysiology Research and Training Center, Faculty of Medicine, Chiang Mai University, Department of Oral Biology and Diagnostic Sciences, Faculty of Dentistry, Chiang Mai University, Chiang Mai, 50200, Thailand.
E-mail address: siriporn.c@cmu.ac.th (S.C. Chattipakorn).

https://doi.org/10.1016/j.lfs.2019.116878
Received 24 July 2019; Received in revised form 10 September 2019; Accepted 13 September 2019
Available online 31 October 2019
0024-3205/

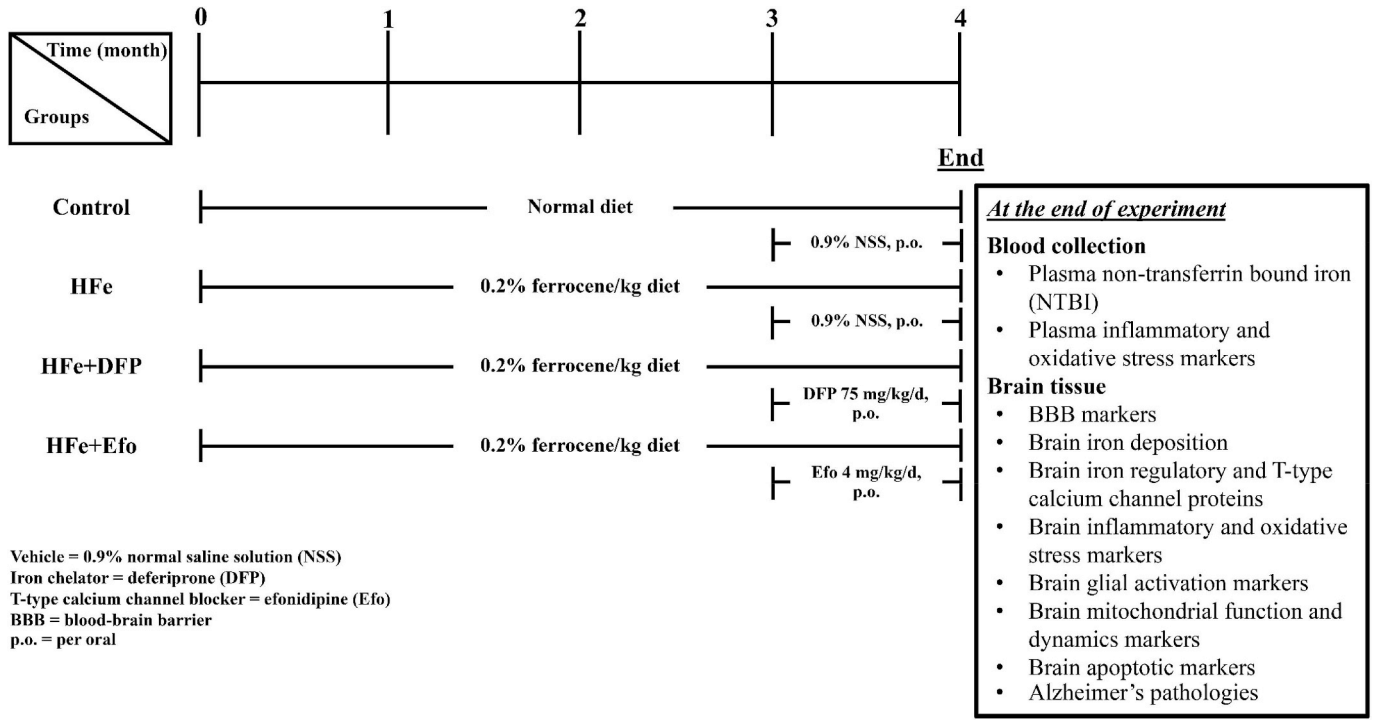

Fig. 1. The summary of experimental protocol for both wild-type and heterozygous mice. DFP; deferiprone; Efo; efonidipine; HFe; high-iron diet, ND; normal diet.

toxicity in iron-overload thalassemic animals has not been investigated. Furthermore, several studies also positively showed a correlation between brain iron-overload and microglia hyperactivation which is accompanied with neuroinflammation [9–11], and increased brain oxidative stress [10]. However, there is little known about the effect of microglia hyperactivation following thalassemic condition with iron-overload.

The beneficial effects of deferiprone therapy in the heart of thalassemic patients have been reported [12–14]. However, there was no report revealing the usefulness of deferiprone against brain toxicity of thalassemic patients.

Recently, a T-type calcium channel (TTCC) blocker (efonidipine) has been reported to exert cardioprotective effects in thalassemic mice with iron-overload [15,16]. These findings indicate that TTCC might also play an important role in brain dysfunction of thalassemic condition. Nevertheless, there is no study demonstrating the potential role of TTCC in the brain of thalassemic condition with iron-overload.

Therefore, we hypothesized that 1) brain toxicity in iron-overload condition was demonstrated by elevated iron accumulation, circulating/brain inflammation, circulating/brain oxidative stress, blood-brain-barrier (BBB) breakdown, the expression of brain divalent metal transporter-1 and T-type calcium channel, glial hyperactivation, brain mitochondrial dysfunction, imbalance of brain mitochondrial dynamics, brain apoptosis, and Alzheimer's like changes, in both wild-type and thalassemic mice, and 2) not only deferiprone, but also efonidipine, provides neuroprotection against iron toxicity in wild-type and thalassemic mice.

2. Materials and methods

2.1. Animal model

Adult C57/BL6 mice (3–6 months old (20–25 g); n = 64) including wild-type (mu$\beta^{+/+}$, WT n = 32) and heterozygous β-Knockout type (mu$\beta^{th\text{-}3/+}$, HT n = 32) were used [17,18]. The HT mice naturally have mild anemia presenting as a decrease in hemoglobin level, an increase in serum iron and reactive oxygen species production, and a decrease in heart rate variability (HRV). These complications are similar to those of thalassemia intermedia observed in humans [19]. Mice were provided by the Thalassemia Research Center, Institute of Molecular Biosciences, Mahidol University, Bangkok, Thailand. All experimental protocols were approved by the Institutional Animal Care and Use Committee from the Faculty of Medicine, Chiang Mai University (13/2560). Mice were housed in well-controlled conditions including 20–22 °C and 50 ± 10% of humidity with a 12-h day/night cycle. Mice had unlimited access to drinking water throughout the entire experiment.

2.2. Iron-overload induction and pharmacological administration

WT and HT mice used as control groups were given a normal diet (ND, n = 8 in both subgroup), whilst all the iron-overload groups were given a diet containing 0.2% ferrocene/kg of diet (HFe, n = 8 in each of 6 subgroups) for 3 consecutive months [15,20]. At the end of the 2-month period, both ND groups were given 0.9% NSS via intragastric gavage, once daily. In contrast, each HFe group received the therapeutic interventions [15,20,21]. These were: 1) HFe mice treated with NSS (HFe control group), 2) HFe mice treated with deferiprone (HFe + DFP), and 3) HFe mice treated with efonidipine (HFe + Efo). HFe + DFP mice received 75-mg/kg/day DFP (Ferriprox®, Apotex Inc., Toronto, Ontario, Canada), via intragastric gavage, twice daily. HFe + Efo mice received 4-mg/kg/day efonidipine (Sigma-Aldrich, St. Louis, MO, USA), via intragastric gavage, once daily. Deferiprone is a commercially available solution (Ferriprox®, Apotex Inc., Toronto, Ontario, Canada), whereas efonidipine compound was dissolved in 0.9% NSS. Mice were given the assigned interventions for 1 month whilst still being fed with the assigned diet. At the end of the experiments (4 months after diet consumption and treatment), all mice were sacrificed, and blood was collected from the heart and kept in Na-heparin tube until further analyses. In addition, brain samples were also collected for further analysis. Plasma was obtained by centrifugation (3000 rpm, 4 °C for 15 min) and subsequently kept frozen at -80 °C until further analysis, tests including those for transferrin bound iron (NTBI), a plasma oxidative stress marker (8-isoprostane) and a plasma inflammatory marker (TNF-α).

After decapitation, brain tissue, apart from the cerebellum, was immediately removed. Brain samples were collected for determining brain parameters including brain iron deposition which was assessed by Prussian blue staining, and presence of brain oxidative stress and brain inflammatory markers. In addition, expression of tight junction proteins in the blood-brain barrier, brain iron-regulatory proteins, brain apoptotic signaling, brain mitochondrial fusion and fission, and glial activation markers. Alzheimer's like pathologies were also determined. The experimental protocol is summarized in Fig. 1.

3. Assessment of plasma non-transferrin bound iron (NTBI)

As modified from a previous study [22], a nitrilotriacetic acid disodium salt (NTA) chelating technique was used. Briefly, plasma was incubated with NTA solution for 30 min to allow Fe^{3+}-$(NTA)^2$ formation [8,15]. The complex from plasma mixture was isolated through a membrane filter (NanoSep®, polysulfone type; Pall Life Sciences, Ann Arbor, MI, USA). The concentration of Fe^{3+}-$(NTA)^2$ was used to calculate the level of NTBI in the ultrafiltrate. Plasma NTBI concentration was detected by flow cytometry (Guava EasyCyte HT, Merck Millipore, Germany).

4. Plasma and brain 8-isoprostaglandin F2α (8-isoprostane) level

The 8-isoprostane level in plasma and brain samples was quantified using Oxiselect™ 8-iso-Prostaglandin F2α ELISA kit (STA-337) (Cell Biolabs, Inc, San Diego, CA, USA. Samples were hydrolyzed (20 µl 10 N NaOH:80 µl sample) at 45 °C for 2 h, then neutralized with 20 µl 10 N HCl to provide a milky product. All samples were subsequently centrifuged at 12,000 g for 5 min. Clear supernatant was used immediately or stored at −20 °C for further analysis. The assay protocol was conducted following manufacturer's procedures. Absorbance was read at a wavelength of 450 nm.

5. Plasma and brain inflammatory markers

Plasma and brain inflammatory markers were investigated using a mouse TNF-α high sensitivity ELISA kit (Invitrogen, CA, USA) in accordance with the protocol detailed by the manufacturer. Absorbance was determined at a wavelength of 450 nm, with the correction wavelength set at 540 nm. Data were expressed in pg/ml unit.

6. Brain iron content assay

Brain homogenate was precipitated in protein precipitation solution (1:1) [7,8]. After centrifugation, supernatants were either mixed in 1.5 mol/l sodium acetate with 0.1% TGA for the blank or in chromogen solution (1:1). Samples were incubated for 30 min at room temperature. Absorbance of samples was investigated at a wavelength of 562 nm.

7. Brain iron deposition assay

Perl's super vital dye solution [8] was used to determine deposition of iron in the brain. Perl's stained tissue was observed under a light microscope (Olympus Corporation, Philadelphia USA) and captured using a camera (Sony, Japan) [8].

8. Amyloids-β 42 (Aβ42) assay

Aβ42 level was measured using mouse Aβ42 sandwich enzyme-linked immunosorbent assay (ELISA) kits (Invitrogen, CA, USA) in accordance with the protocol detailed by the manufacturer. Absorbance was determined at a wavelength of 450 nm and results expressed in pg/mg of protein.

9. Brain mitochondrial isolation technique

Brain mitochondrial isolation was performed as modified from previous studies [23,24]. Mitochondrial pellets were re-suspended with respiration buffer. The protein concentration was determined according to the Bicinchoninic Acid (BCA) Assay as previously described [25].

10. Assessment of brain mitochondrial swelling

Brain mitochondrial swelling was measured by determining the changes in the absorbance of the suspension at 540 nm. Brain mitochondrial swelling was represented by a reduction of absorbance value [7,24].

11. Assessment of brain mitochondrial membrane potential ($\Delta\Psi_m$)

A JC-1 dye was used to determine brain mitochondria membrane potential (ΔΨm) [7,24]. A decreased red/green fluorescence intensity ratio was used to assess brain mitochondrial depolarization [7,24].

12. Determination of brain mitochondrial ROS production

Brain mitochondrial ROS production was measured using fluorescent dichlorohydro-fluorescein diacetate (DCFH-DA) dye. Fluorescence intensity was determined, increased fluorescence intensity indicating an increased brain mitochondrial ROS production [7,24].

13. Immunoblotting assay

Brain protein extraction was prepared by using a lysis buffer composed of 1-mM EDTA, 1-mM EGTA, 1% NP-40, 1% Triton X-100 with 1X protease inhibitor [7]. Total protein (50–80 µg) was mixed with a loading buffer (5% β-mercaptoethanol, 0.05% bromophenol blue, 75 mM Tris-HCl (pH 6.8), 2% SDS and 10% glycerol) and the equal amount of protein from each sample (15 µl/lane) were loaded onto 10% sodium dodecyl sulfate (SDS)-Acrylamide gels (SDS-PAGE). Then, proteins were transferred to a nitrocellulose membrane in a Wet-Tank immunoblotting system (Bio-Rad Laboratories, Hercules, California, USA). The transfer of protein from gel to membrane was confirmed by using Ponceau S solution (Sigma-Aldrich, St. Louis, MO, USA). All membranes were blocked with either 5% skimmed milk or 5% bovine serum albumin (BSA) in 1X-Tris-Buffered Saline and Tween (TBST) buffer for 1 h at room temperature. Membranes were subsequently exposed to primary antibodies for specific protein identification including: 1) tight junction protein at the blood-brain barrier, occludin (SC-5562, Santa Cruz Biotechnology, Santa Cruz, CA, USA) and claudin-5 (ab15106, Abcam, Cambridge, UK); 2) glial markers, glial fibrillary acidic protein (GFAP) (#3670S, Cell Signaling Technology, Danvers, MA, USA) and cluster of differentiation 68 (CD68) (ab125212, Abcam, Cambridge, UK); 3) apoptotic markers, bax (ab182733, Abcam, Cambridge, UK) and bcl-2 (ab196495, Abcam, Cambridge, UK); 4) the iron transporter, divalent metal transporter 1 (DMT-1) (ab55812, Abcam, Cambridge, UK); 5) mitochondrial fusion markers, optic atrophy-1 (OPA-1) (#80471S, Cell Signaling Technology, Danvers, MA, USA) and mitofusin-2 (Mfn2) (#9482, Cell Signaling Technology, Danvers, MA, USA); 6) mitochondrial fission markers, dynamin-related protein 1 (Total-DRP1) (#5391, Cell Signaling Technology, Danvers, MA, USA) and its phosphorylated form (p-$DRP1_{Ser616}$) (#3455, Cell Signaling Technology, Danvers, MA, USA); 6) Alzheimer's like pathologies, tau (#4019, Cell Signaling Technology, Danvers, MA, USA) and its phosphorylated form (p-Tau_{Thr181}) (#12885, Cell Signaling Technology, Danvers, MA, USA), β-amyloid (SC-28395, Santa Cruz Biotechnology, Santa Cruz, CA, USA), and amyloid precursor protein (APP) (#2452, Cell Signaling Technology, Danvers, MA, USA), and 7) β-actin (SC-47778, Santa Cruz Biotechnology, Santa Cruz, CA, USA). All these were kept overnight at 4 °C. Protein bands were visualized using ECL western

blotting detection reagent. Densitometry analysis of bands were measured by Image Processing and Analysis in Java (ImageJ) program (NIH, Bethesda, MD) and represented in average of signal intensity (arbitrary units).

13.1. Data analysis

Data were expressed as mean ± standard error of mean (SEM). One-way ANOVA followed by a least-significance difference (LSD) post-hoc test analysis was used for a comparison between the groups. Student's t-tests were used for paired comparisons. P-value < 0.05 was considered statistically significant.

14. Results

14.1. Chronic HFe diet consumption induced circulating iron-overload, oxidative stress, and inflammation and T-type calcium channels are possible portals for brain iron uptake

Chronic HFe consumption induced a circulation iron-overload condition in both wild-type (WT) and heterozygous thalassemic (HT) mice to an equal extent, as demonstrated by an increased plasma NTBI (Table 1). In addition, oxidative stress and inflammation were observed in HFe-fed WT and HT mice, as demonstrated by an elevation in plasma levels of 8-isoprostane and TNF-α (Table 1).

Despite the pathological changes in circulation, HFe consumption also potentially induced a loss of blood-brain barrier (BBB) integrity in both WT and HT mice, as indicated by a decreased expression of tight junction proteins at the BBB (claudin-5 and occludin) (Fig. 2A and B). An elevation in brain iron accumulation was also observed to a significant level in both HFe-fed WT and HT mice (Fig. 2C). Interestingly, there was an up-regulation of T-type calcium channel (TTCC) expression in HFe-fed WT and HT mice (Fig. 2D). Nonetheless, the protein expression of brain iron transporter divalent metal transporter-1 (DMT-1) in HFe-fed WT and HT mice showed no change in comparison to that of ND-fed WT and HT mice (Fig. 2E). Regarding the brain iron deposition, we found that the iron deposition was sporadically occurred in the brain (Fig. 3A). However, we found that iron accumulation was noticed in pyramidal cells of hippocampus (Fig. 3B). All of these findings demonstrate that brain TTCC may be a route for brain iron accumulation during conditions of iron-overload.

14.2. Administration of an iron chelator or TTCC blocker attenuated circulating iron-overload, oxidative stress, and inflammation in both HFe-fed WT and HT mice

With regards to pharmacological interventions, both the iron chelator: deferiprone, and T-type calcium channel blocker: efonidipine, alleviated the pathological condition induced by iron-overload as indicated by a reduction in plasma NTBI, plasma 8-isoprostane and plasma TNF-α (Table 2). These findings suggest that both the iron chelator and TTCC blocker had equal impact on reducing circulation pathologies caused by the iron-overload condition.

14.3. Circulating iron-overload condition induced the reduction of blood-brain barrier (BBB) integrity, and increased brain iron accumulation, which were restored by a specific iron chelator and TTCC blocker

An iron-overload condition led to a reduction in BBB integrity, an increase in brain TTCC expression, and brain iron accumulation in both HFe-fed WT and HT mice. Interestingly, both deferiprone and efonidipine effectively restored BBB disruption in both HFe-fed WT and HT mice (Fig. 4A and B). Moreover, a reduction in TTCC expression in HFe-fed WT and HT mice following both interventions was observed (Fig. 4C). There was no change in brain DMT-1 expression in all groups (Fig. 4D). Both deferiprone and efonidipine also prevented brain iron accumulation in HFe-fed WT and HT mice (Fig. 4E). Consistent with brain iron level, administration of both deferiprone and efonidipine could prevent brain iron deposition in whole brain section (Fig. 5A) and hippocampus (Fig. 5B).

14.4. Circulating iron-overload equally induced brain oxidative stress, brain inflammation, and glial hyperactivation in both HFe-fed WT and HT mice which could be prevented by both interventions

Brain 8-isoprostane and brain TNF-α were elevated in HFe-fed WT and HT mice, when compared with ND-fed WT and HT mice (Fig. 6A and B). Glial hyperactivation was also observed, as indicated by the up-regulation in protein expression of cluster differentiation 68 (CD68) and glia fibrillary acidic protein (GFAP), microglial and astrocytic markers, respectively (Fig. 6B–D). These findings suggest that circulating iron-overload not only induces pathological changes in the peripheral area, but also causes brain pathologies including brain iron-overload, brain oxidative stress, brain inflammation, and glial hyperactivation. Interestingly, both deferiprone and efonidipine treatments provided equal efficacy in restoring brain oxidative stress, brain inflammation, and the up-regulated glial protein expression (Fig. 6).

14.5. Circulating iron-overload induced brain apoptosis, impaired brain mitochondrial function, and disrupted brain mitochondrial dynamics, but both interventions prevented brain cell death and attenuated brain mitochondrial changes in both HFe-fed WT and HT mice

Circulating iron-overload could also induce brain mitochondrial dysfunction by increasing brain mitochondrial reactive oxygen species (ROS) production, indicated by a decreasing red/green fluorescent intensity ratio which typifies brain mitochondrial depolarization, and reducing absorbance of mitochondrial suspension which demonstrated brain mitochondrial swelling (Fig. 7A–C). Although there was no change in the total formation of dynamin related protein-1 (Total-DRP-1) expression (Fig. 7D), phosphorylated dynamin related protein-1 at serine 616 (p-DRP-1_{Ser616}) was up-regulated in HFe-fed WT and HT mice (Fig. 7E), indicating the elevation of the mitochondrial fission process. On the other hand, mitofusin-2 (Mfn2) and optic atrophy 1 (OPA1) were decreased in HFe-fed WT and HT mice (Fig. 7F and G), demonstrating the reduction of mitochondrial fusion. These findings indicate that iron-overload could unbalance the processes involved in brain mitochondrial dynamics (Fig. 7C–G). Surprisingly, both interventions potentially prevented brain mitochondrial dysfunction and the

Table 1
Effects of high-iron diet consumption on plasma iron-overload, oxidative stress, and inflammation.

Peripheral parameters	Wild-type mice (WT)		Heterozygous mice (HT)	
	ND	HFe	ND	HFe
Plasma NTBI (μM)	0	4.19 ± 0.26*	0	4.21 ± 0.49*
Plasma 8-isoprostane (ng/ml)	6.36 ± 2.10	52.23 ± 4.55*	5.96 ± 2.05	54.58 ± 3.78*
Plasma TNF-α (pg/ml)	6.01 ± 0.11	8.40 ± 0.96*	6.03 ± 0.20	9.16 ± 0.59*

*p < 0.05 vs. ND group. HFe; high-iron diet, ND; normal diet, NTBI; non-transferrin bound iron, TNF-α; tumor necrosis factor-alpha.

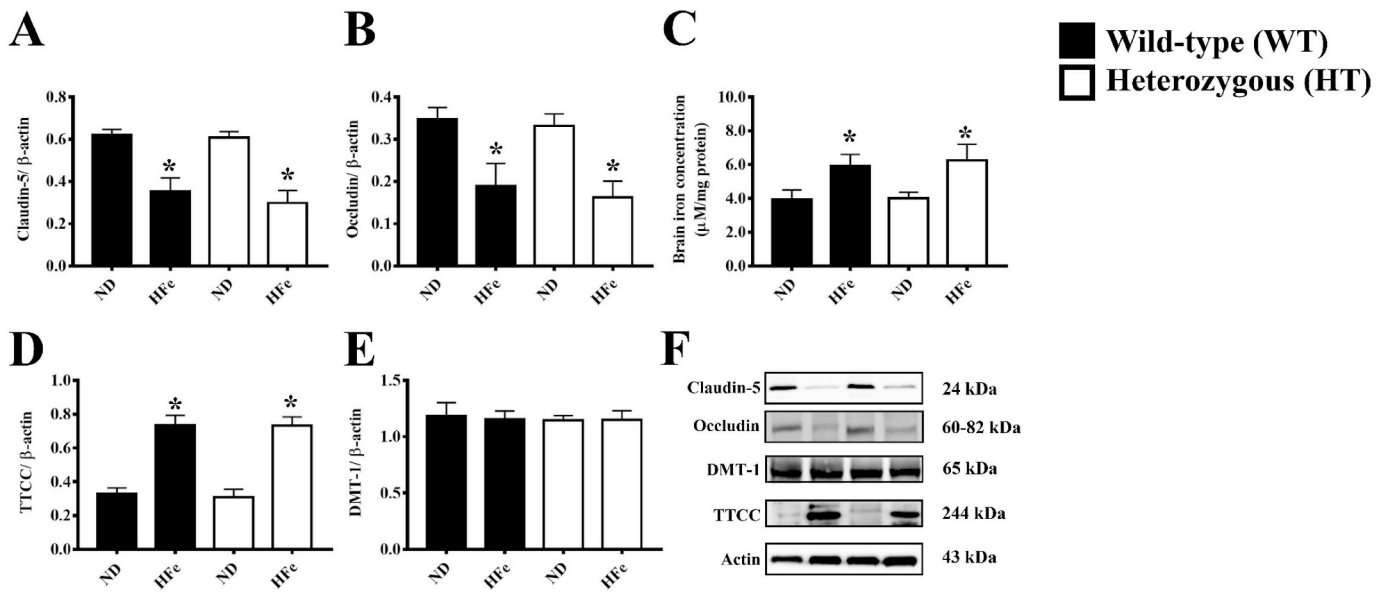

Fig. 2. Effects of chronic high-iron diet consumption on tight junction proteins of blood-brain barrier (A and B); brain iron level (C); brain t-type calcium channels (D); and brain iron transporters (E). Representative bands of tight junction proteins, brain t-type calcium channels, and brain iron transporters are shown in panel F. Experimental group from each lane includes 1. WT-ND, 2. WT-HFe, 3. HT-ND, and 4. HT-HFe. *$p < 0.05$ vs ND group. DMT-1; divalent metal transporter-1, HFe; high-iron diet, HT; heterozygous mice, ND; normal diet, TTCC; t-type calcium channel, WT; wild-type mice.

imbalance of brain mitochondrial dynamics (Fig. 7).

In addition, the iron-overload condition triggered the up-regulated expression of a pro-apoptotic protein (bax) (Fig. 8A) and the elevated apoptosis ratio (Fig. 8C) in both HFe-fed WT and HT mice, although the anti-apoptotic protein expression did not change (Fig. 8B). These suggest that iron overload potentially induced brain apoptosis. However, both pharmacological treatments effectively prevent brain impairment from iron-induced brain apoptosis, when compared with HFe-fed WT and HT mice (Fig. 8).

Taken together, these findings suggest that iron-overload induced brain apoptosis and brain mitochondrial alteration and the administration of an iron chelator and a calcium channel blocker protected the brain against brain mitochondrial changes.

14.6. Circulating iron-overload induced β-amyloid accumulation and tau hyperphosphorylation, but an iron chelator and a TTCC blocker decreased the occurrence of these Alzheimer's-like pathologies in both HFe-fed WT and HT mice

There was an increase in β-amyloid level and protein expression in HFe-fed WT and HT mice (Fig. 9A and B), in association with a reduction in amyloid-precursor protein (APP) (Fig. 9C). Iron-overload also induced a hyperphosphorylation of tau protein at Threonine 181 (Fig. 9D), although total-tau protein expression was not changed (Fig. 9E). Nonetheless, these potentially serious effects were abolished when deferiprone or efonidipine were administered in both HFe-fed WT and HT mice (Fig. 9). These findings demonstrate that iron-overload led to an increase the Alzheimer's like changes and both interventions effectively, equally, hindered this deleterious effect.

15. Discussion

The major findings from this study are as follows: 1) chronic HFe consumption equally induced pathological conditions in peripheral areas of both HFe-fed WT and HT mice by inducing circulation iron-overload, oxidative stress, and inflammation; 2) TTCC may be a possible route for brain iron uptake under conditions of circulating iron-overload, leading to BBB breakdown, brain iron accumulation, brain iron deposition, brain oxidative stress, brain inflammation, glial hyperactivation, brain mitochondrial changes as regards both function and dynamics, brain apoptosis, and Alzheimer's like pathologies; 3) the iron chelator, deferiprone, and the TTCC blocker, efonidipine, equally attenuated circulating changes by mitigating circulating iron-overload, oxidative stress, and inflammation, and 4) deferiprone and efonidipine also exhibited equal efficacy in neuroprotection by providing restorative effects on BBB integrity, TTCC protein expression, brain iron

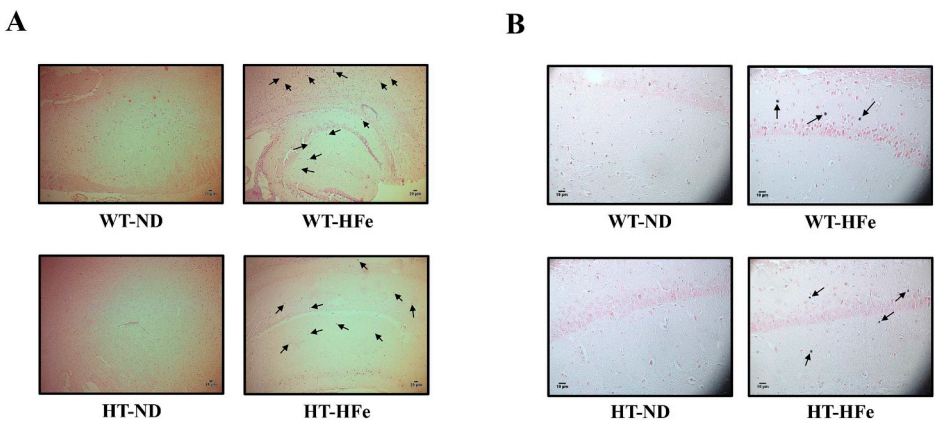

Fig. 3. Representative images of Prussian blue iron staining in whole brain section (A) and hippocampus (B) of wild-type and thalassemic mice using with 5X and 20X magnification objective lens, respectively. Arrows indicate blue-colored iron staining in brain. HFe; high-iron diet, HT; heterozygous mice, ND; normal diet, WT; wild-type mice. (For interpretation of the references to color in this figure legend, the reader is referred to the Web version of this article.)

Table 2
Effects of pharmacological interventions on peripheral parameters.

Peripheral parameters	Wild-type mice (WT)				Heterozygous mice (HT)			
	ND	HFe	HFe + DFP	HFe + Efo	ND	HFe	HFe + DFP	HFe + Efo
Plasma NTBI (μM)	0	4.17 ± 0.22*	2.95 ± 0.18*,†	2.52 ± 0.40*,†	0	4.17 ± 0.42*	3.10 ± 0.19*,†	3.06 ± 0.29*,†
Plasma 8-isoprostane (ng/ml)	7.35 ± 1.98	44.28 ± 9.65*	16.94 ± 3.17*,†	10.76 ± 4.76*,†	6.13 ± 1.69	55.32 ± 3.02*	32.04 ± 8.16*,†	23.77 ± 7.81*,†
Plasma TNF-α (pg/ml)	5.96 ± 0.08	8.10 ± 0.74*	7.21 ± 0.16*,†	6.98 ± 0.14*,†	6.05 ± 0.15	9.21 ± 0.83*	7.70 ± 0.04*,†	7.90 ± 0.47*,†

*p < 0.05 vs. ND group, †p < 0.05 vs HFe group. DFP; deferiprone, Efo; efonidipine, HFe; high-iron diet, ND; normal diet, NTBI; non-transferrin bound iron, TNF-α; tumor necrosis factor-alpha.

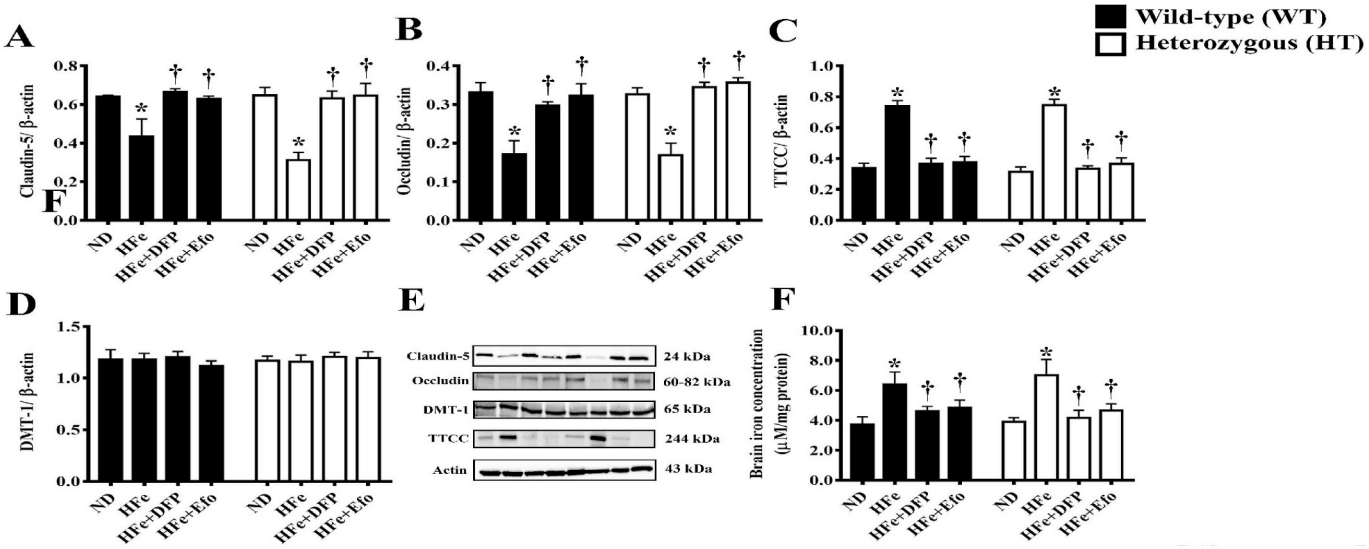

Fig. 4. Effects of deferiprone and efonidipine on tight junction proteins of blood-brain barrier (A and B); brain t-type calcium channel (C); brain iron transporter (D); and brain iron level (F). Representative bands of tight junction proteins, brain t-type calcium channels, and brain iron transporters are shown in panel E. Experimental group from each lane includes 1. WT-ND, 2. WT-HFe, 3. WT-HFe + DFP, 4. WT-HFe + Efo, 5. HT-ND, 6. HT-HFe, 7. HT-HFe + DFP, and 8. HT-HFe + Efo. *p < 0.05 vs ND group, †p < 0.05 vs HFe group. DFP; deferiprone, DMT-1; divalent metal transporter-1, Efo; efonidipine, HFe; high-iron diet, HT; heterozygous mice, ND; normal diet, TTCC; t-type calcium channel, WT; wild-type mice.

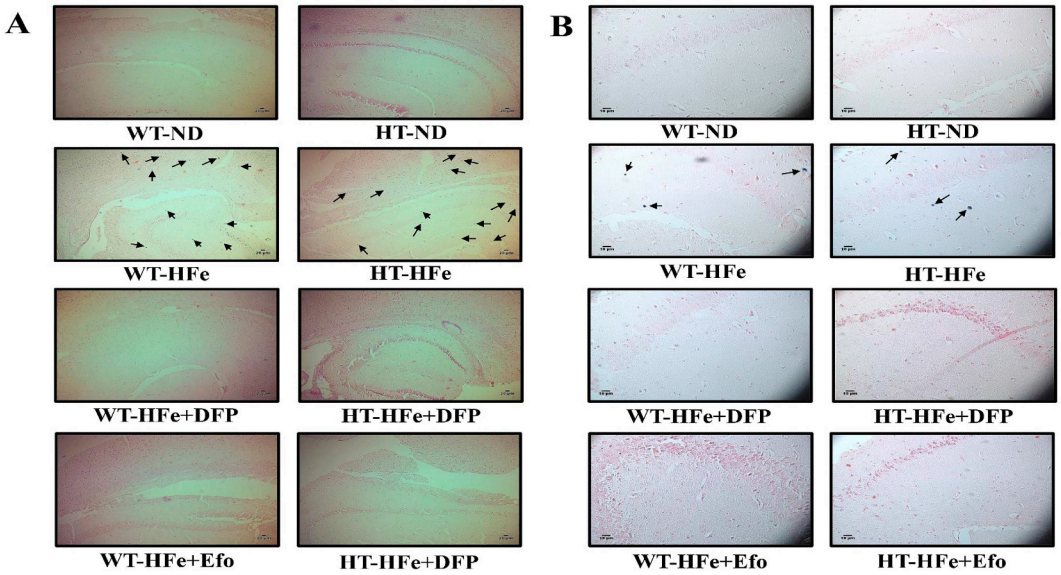

Fig. 5. Representative images of Prussian blue iron staining in whole brain section (A) and hippocampus (B) of wild-type and thalassemic mice using with 5X and 20X magnification objective lens, respectively. Arrows indicate blue-colored iron staining in brain. Treatment with either DFP or Efo protected brain against iron deposition. DFP; deferiprone, Efo; efonidipine, HFe; high-iron diet, HT; heterozygous mice, ND; normal diet, WT; wild-type mice. (For interpretation of the references to color in this figure legend, the reader is referred to the Web version of this article.)

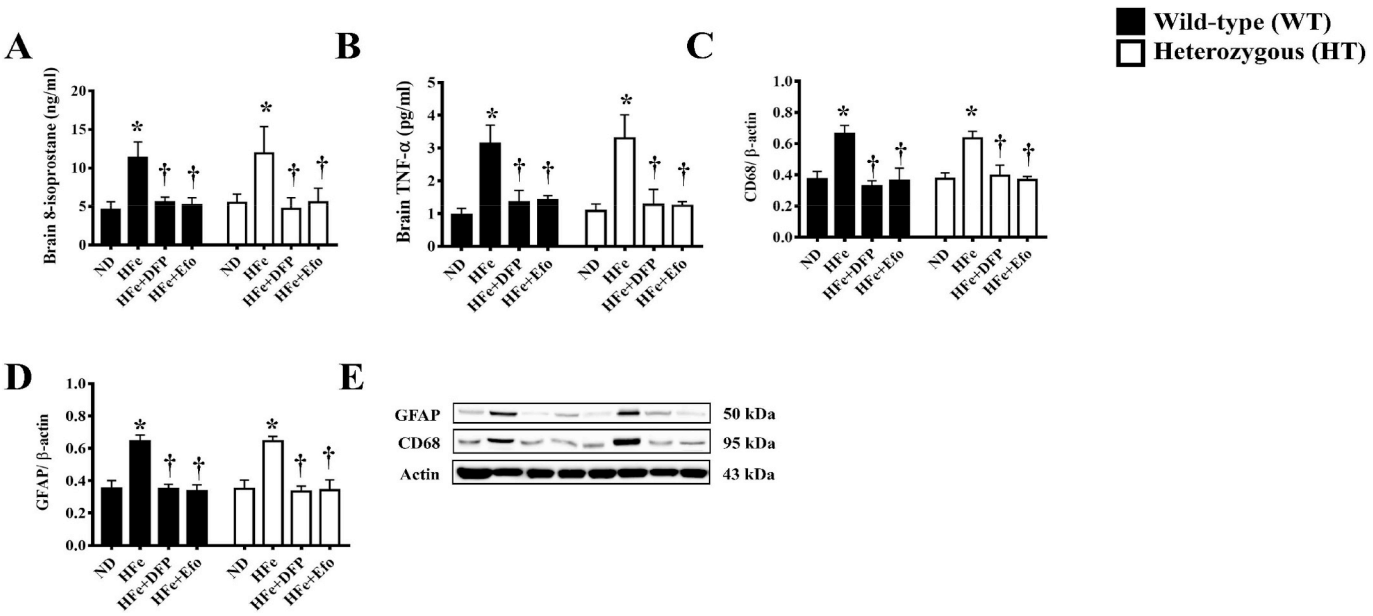

Fig. 6. Effects of deferiprone and efonidipine on brain oxidative stress (A), brain inflammation (B), microglial activation (C), and astrocytic activation (D). Representative bands for the activation of microglia and astrocyte are shown in panel E. $^{*}p < 0.05$ vs ND group, $^{\dagger}p < 0.05$ vs HFe group. Experimental group from each lane includes 1. WT-ND, 2. WT-HFe, 3. WT-HFe + DFP, 4. WT-HFe + Efo, 5. HT-ND, 6. HT-HFe, 7. HT-HFe + DFP, and 8. HT-HFe + Efo. CD68; cluster of differentiation 68, DFP; deferiprone, Efo; efonidipine, GFAP; glial fibrillary acidic protein, HFe; high-iron diet, ND; normal diet, TNF-α; tumor necrosis factor-alpha.

content, brain oxidative stress, brain inflammation and glial hyperactivation, brain mitochondrial function, brain mitochondrial dynamics, brain apoptosis, and Alzheimer's like changes.

Consistent with our previous report, this study found that the severity of circulating iron-overload occurred equally in both HFe-fed WT and HT mice [15]. This might be due to the circulating iron-overload by chronic consumption of HFe for 4 months would be at the maximum level of iron-overload, hence induced the most severe level of iron toxicity. Therefore, the peripheral and brain pathologies were no different between HFe-fed WT and HFe-fed HT mice. Nonetheless, this is the first study to demonstrate that the circulating iron-overload induced brain pathologies in thalassemic mice and the pharmacological interventions using iron chelator and calcium channels blocker effectively provided neuroprotection against iron-overload conditions in a thalassemic model.

Divalent metal transporter 1 (DMT-1) is commonly known as physiological pathway for iron entry into the cells, particularly in brain cells [26,27]. A recent study revealed that an increased expression of DMT1 in both mRNA and protein lead to enhances uptake of Fe^{2+} in C6 glioma cells [28]. This finding suggested that an increase in DMT-1 expression was associated with brain iron accumulation. However, we found that under conditions of iron-overload, the protein expression of DMT-1 was not changed in iron-overload WT and HT mice, when compared with control mice. This inconsistency might be due to several possibilities including: 1) the severity of iron overload was insufficient to alter this protein expression; 2) under iron-overload, DMT-1 was

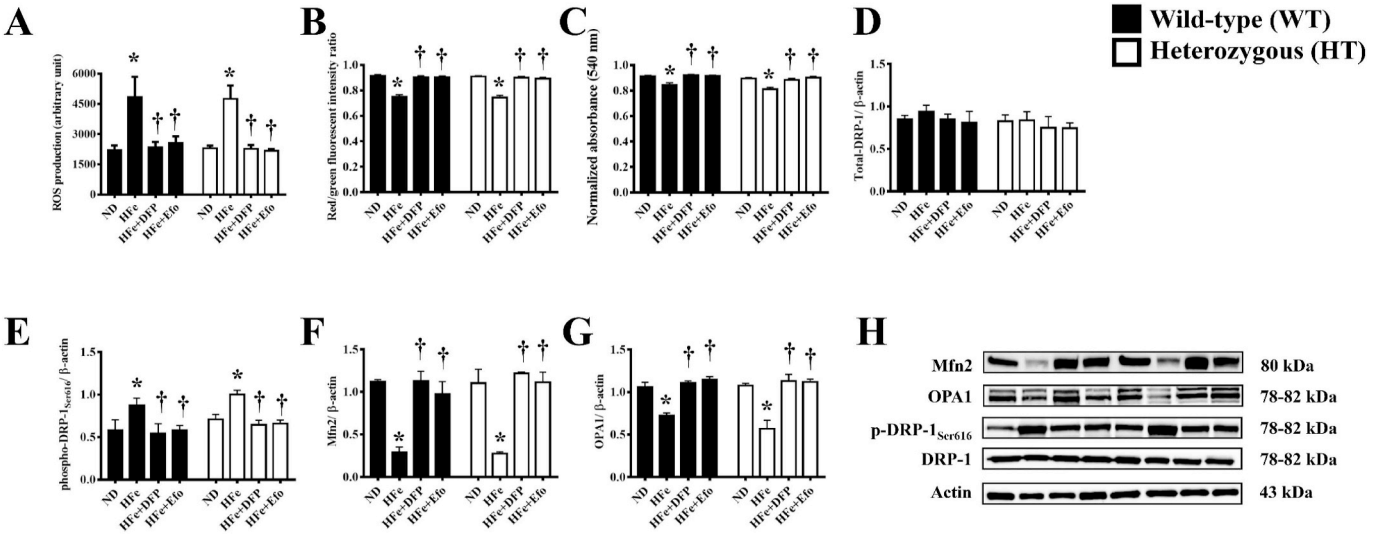

Fig. 7. Effects of deferiprone and efonidipine on: brain mitochondrial ROS production (A), mitochondrial membrane potential change (B), mitochondrial swelling (C), mitochondrial fission proteins (D and E), and mitochondrial fusion proteins (F and G). Representative bands for mitochondrial fission and fusion proteins are shown in panel H. Experimental group from each lane includes 1. WT-ND, 2. WT-HFe, 3. WT-HFe + DFP, 4. WT-HFe + Efo, 5. HT-ND, 6. HT-HFe, 7. HT-HFe + DFP, and 8. HT-HFe + Efo. $^{*}p < 0.05$ vs ND group, $^{\dagger}p < 0.05$ vs HFe group. DFP; deferiprone, DRP-1; dynamin-related protein 1, Efo; efonidipine, HFe; high-iron diet, Mfn2; mitofusin 2, ND; normal diet, OPA1; optic atrophy 1, ROS; reactive oxygen species.

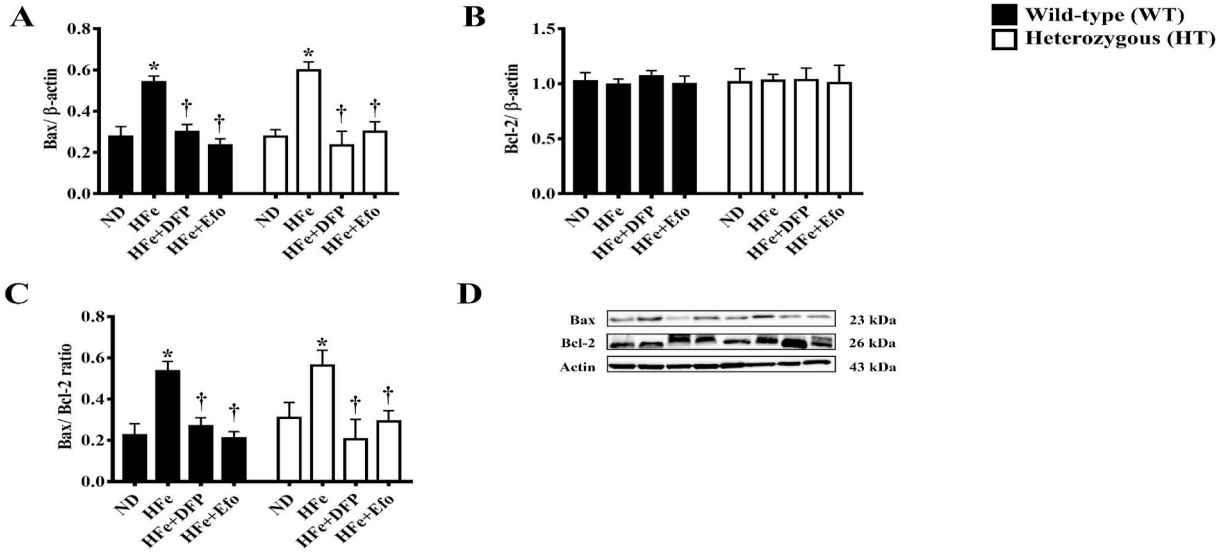

Fig. 8. Effects of deferiprone and efonidipine on brain apoptotic markers; bax (A), anti-apoptotic markers; bcl-2 (B), and apoptotic ratio (C). Representative bands for apoptotic-related proteins are shown in panel E. Experimental group from each lane includes 1. WT-ND, 2. WT-HFe, 3. WT-HFe + DFP, 4. WT-HFe + Efo, 5. HT-ND, 6. HT-HFe, 7. HT-HFe + DFP, and 8. HT-HFe + Efo. $^{*}p < 0.05$ vs ND group, $^{\dagger}p < 0.05$ vs HFe group. DFP; deferiprone, Efo; efonidipine, HFe; high-iron diet, ND; normal diet.

used as one of portals for brain iron uptake, and 3) DMT-1 might not be a major route for iron uptake into the brain, since several studies demonstrated that calcium channels played an important role in the alternative route for brain iron uptake under iron-overload conditions [29–31].

Surprisingly, we found that TTCC protein in the brain was up-regulated following circulating iron-overload caused by chronic HFe consumption. This finding is consistent with recent studies which indicated that the TTCC expression increased and also that TTCCs played a significant role in the cardiac dysfunction in cases of thalassemia with iron-overload conditions [20,32]. Collectively, these findings demonstrate that TTCC might also play an important role in brain complications in thalassemic patients with iron-overload. Therefore, the administration of a TTCC blocker could be considered as one of therapeutic strategies for preventing iron-overload conditions and also iron-induced organs toxicity in these patients.

In the present study, glial hyperactivation in the iron-overload brain was found, as indicated by an up-regulation of microglial and astrocytic markers (CD68 and GFAP, respectively). The hyperactivation of microglia, resulting from an inflammatory response, occurred when neurons were damaged [33,34]. After exposure to the extracellular signals such as pathogens, foreign substances as well as dead cells, morphological changes of microglia can occur into amoeboid shapes which are associated with short processes [35]. Not only were there solely morphological changes but the hyperactivation of microglia also led to changes in both cellular signaling and gene expression. These changes resulted in the release of pro- or anti-inflammatory factors and free radicals and the recruitment of certain molecules [36,37]. Several

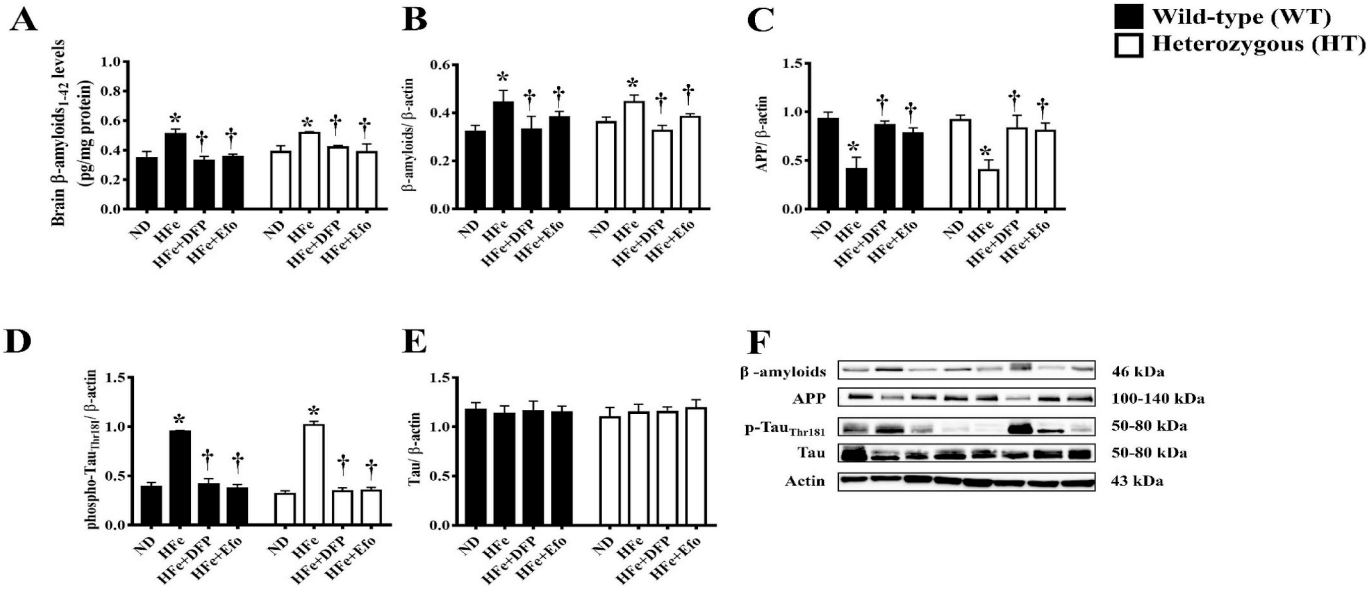

Fig. 9. Effects of deferiprone and efonidipine on brain β-amyloid level (A) and protein expression of β-amyloid (B), amyloid precursor protein (APP) (C), tau proteins (D and E). Representative bands for β-amyloids, APP, and tau proteins are shown in panel F. Experimental group from each lane includes 1. WT-ND, 2. WT-HFe, 3. WT-HFe + DFP, 4. WT-HFe + Efo, 5. HT-ND, 6. HT-HFe, 7. HT-HFe + DFP, and 8. HT-HFe + Efo. $^{*}p < 0.05$ vs ND group, $^{\dagger}p < 0.05$ vs HFe group. APP; amyloid precursor protein, DFP; deferiprone, Efo; efonidipine, HFe; high-iron diet, ND; normal diet.

studies also demonstrated that an over-activation of microglia caused neurotoxicity since they can activate pro-inflammatory factors including IL-1β, TNF-α, and nitric oxide (NO) [38,39].

Not only microglial hyperactivation, astrocytic hyperactivation has been reported which played an important role in neuroinflammation [40,41]. An increased level of several inflammatory cytokines such as IL-1β, IL-6, and TNFα could trigger a classical state of astrocytic hyperactivation [42]. It has been demonstrated that an elevation in the GFAP expression is a hallmark of neuroinflammation-mediated neurodegeneration, particularly in cases of Alzheimer's disease [43]. Furthermore, hyperactivated microglia amplified the hyperactivation of astrocytes through a release of inflammatory cytokines such as IL-1β and TNF-α which effectively induced neuronal injury [44–46].

Glial hyperactivation was also associated with iron-mediated oxidative stress and neuroinflammation [47–50]. Activation of an NADPH oxidase (NOX), a critical enzyme in the ROS-generating system in microglia not only plays a role in neuroinflammation, but also contributes to neuronal death [51–53]. In addition, microglial phagocytic inability to clear abnormally aggregated Aβ could lead to the induction of inflammation, oxidative stress, and neurodegeneration [54–56]. Astrocytes were also involved in the incidence of oxidative stress [57]. The β-amyloid treatment increased an intracellular-free Ca^{2+} influx from the extracellular space which activated nitric oxide NADPH oxidase (NOX), leading to induced astrocytic mitochondrial dysfunction [57]. Furthermore, a recent study reported that under conditions of oxidative stress a neuronal glycolytic metabolic pattern was altered, as demonstrated by a reduction in glutamate-glutamine cycling between the neurons and the astrocytes [48]. Astrocytic cell proliferation was increased to counter the metabolic shift and provide sufficient energy substrates to neuronal cells [48]. Consistent with these previous studies, brain inflammation and brain oxidative stress were also observed in the present study. Taken altogether these findings suggest that the hyperactivation of microglia and astrocytes, in response to peripheral and central iron-stimuli, led to an increase in inflammatory cytokines and oxidative stress in brain and thus subsequently inducing neuronal injury.

Regarding the pharmacological interventions, the iron chelator, deferiprone, exerted neuroprotective effects in the thalassemic model with iron-overload. Although this is the first study indicating the protective effects on the brain of thalassemic subjects, its neuroprotective effects have also been recently reported in iron-overload rats [7,8].

Separate to the action of the iron chelator, we found that a TTCC blocker, efonidipine, potentially attenuated the iron-overload condition in both circulations impacted and brain regions of WT and HT mice fed with HFe. To explain the underlying mechanism responsible for these findings, some studies have reported that the carbonyl group in the chemical structure of efonidipine which confer the efficacy for iron chelation [58,59]. In addition, efonidipine also reduced the plasma oxidative stress caused by HFe consumption. A recent report indicated an anti-oxidant effect of efonidipine in an acute renal failure rat model [60]. This implied that efonidipine administration could be either prevent iron uptake into the brain or have a direct effect on reducing iron-induced oxidative stress. Taken together, these findings support a reason why this TTCC blocker effectively attenuated circulating iron-overload and other complications associated with circulation, resulting in protection of the brain against iron toxicity as demonstrated in this study. However, further investigation is still required to clarify its underlying mechanisms as a neuroprotective agent under iron-overload conditions.

In conclusion, the iron-overload condition plays an important role in causing brain toxicity in not only the thalassemic model, but also a wild-type model. Interestingly, the administration of an iron chelator and a T-type calcium channel blocker exerted neuroprotective effects of equal magnitude against the iron-overload condition through several underlying mechanisms. Taken together, these findings suggest that iron chelation and calcium channel blocking could be potential strategies for neuroprotection from iron-overload condition in thalassemic patients.

Study limitation

Regarding the pharmacological inventions, it would be very interesting to see dose-dependent activity and may be the higher dose could provide better activity.

Author contributions

Conceived and designed the experiments: JS NC SC. Performed the experiments: JS JK. Analyzed the data: JS. Contributed reagents/materials/analysis tools: SS SSri SF NC SC. Wrote the paper: JS NC SC. Critical review of the article: JS NC SC.

Declarations of competing interest

None.

Acknowledgement

This work was supported by Thailand Research Fund Grants TRF-RTA6080003 (SCC) and MRG6080226 (JS), the Faculty of Medicine Chiang Mai University Endowment Fund: 001–2561 (JS), a NSTDA Research Chair Grant from the National Science and Technology Development Agency Thailand (NC), and a Chiang Mai University Center of Excellence Award (NC).

References

[1] F.D. Armstrong, Thalassemia and learning: neurocognitive functioning in children, Ann. N. Y. Acad. Sci. 1054 (2005) 283–289.
[2] O. Duman, S. Arayici, C. Fettahoglu, N. Eryilmaz, S. Ozkaynak, A. Yesilipek, et al., Neurocognitive function in patients with beta-thalassemia major, Pediatr. Int. 53 (2011) 519–523.
[3] P. Nemtsas, M. Arnaoutoglou, V. Perifanis, E. Koutsouraki, A. Orologas, Neurological complications of beta-thalassemia, Ann. Hematol. 94 (2015) 1261–1265.
[4] Z.M. Qian, Q. Wang, Expression of iron transport proteins and excessive iron accumulation in the brain in neurodegenerative disorders, Brain Res Brain Res Rev 27 (1998) 257–267.
[5] D. Xian-hui, G. Wei-juan, S. Tie-mei, X. Hong-lin, B. Jiang-tao, Z. Jing-yi, et al., Age-related changes of brain iron load changes in the frontal cortex in APPswe/PS1DeltaE9 transgenic mouse model of Alzheimer's disease, J. Trace Elem. Med. Biol. 30 (2015) 118–123.
[6] W. Zheng, N. Xin, Z.H. Chi, B.L. Zhao, J. Zhang, J.Y. Li, et al., Divalent metal transporter 1 is involved in amyloid precursor protein processing and Abeta generation, FASEB J. 23 (2009) 4207–4217.
[7] J. Sripetchwandee, N. Pipatpiboon, N. Chattipakorn, S. Chattipakorn, Combined therapy of iron chelator and antioxidant completely restores brain dysfunction induced by iron toxicity, PLoS One 9 (2014) e85115.
[8] J. Sripetchwandee, S. Wongjaikam, W. Krintratun, N. Chattipakorn, S.C. Chattipakorn, A combination of an iron chelator with an antioxidant effectively diminishes the dendritic loss, tau-hyperphosphorylation, amyloids-beta accumulation and brain mitochondrial dynamic disruption in rats with chronic iron-overload, Neuroscience 332 (2016) 191–202.
[9] X.F. He, Y. Lan, Q. Zhang, D.X. Liu, Q. Wang, F.Y. Liang, et al., Deferoxamine Inhibits Microglial Activation, Attenuates Blood-Brain Barrier Disruption, Rescues Dendritic Damage and Improves Spatial Memory in a Mouse Model of Microhemorrhages, J Neurochem, 2016.
[10] H. Wu, T. Wu, X. Xu, J. Wang, J. Wang, Iron toxicity in mice with collagenase-induced intracerebral hemorrhage, J. Cereb. Blood Flow Metab. 31 (2011) 1243–1250.
[11] E. Mracsko, R. Veltkamp, Neuroinflammation after intracerebral hemorrhage, Front. Cell. Neurosci. 8 (2014) 388.
[12] A.C. Chen, C.T. Peng, S.F. Wu, K.H. Wu, I.P. Chiang, C.H. Tsai, Effect of deferiprone on liver iron overload and fibrosis in hepatitis-C-virus-infected thalassemia, Hemoglobin 30 (2006) 209–214.
[13] D.J. Pennell, V. Berdoukas, M. Karagiorga, V. Ladis, A. Piga, A. Aessopos, et al., Randomized controlled trial of deferiprone or deferoxamine in beta-thalassemia major patients with asymptomatic myocardial siderosis, Blood 107 (2006) 3738–3744.
[14] A. Piga, C. Gaglioti, E. Fogliacco, F. Tricta, Comparative effects of deferiprone and deferoxamine on survival and cardiac disease in patients with thalassemia major: a retrospective analysis, Haematologica 88 (2003) 489–496.

[15] J. Khamseekaew, S. Kumfu, S. Wongjaikam, S. Kerdphoo, T. Jaiwongkam, S. Srichairatanakool, et al., Effects of iron overload, an iron chelator and a T-Type calcium channel blocker on cardiac mitochondrial biogenesis and mitochondrial dynamics in thalassemic mice, Eur. J. Pharmacol. 799 (2017) 118–127.
[16] S. Kumfu, J. Khamseekaew, S. Palee, S. Srichairatanakool, S. Fucharoen, S.C. Chattipakorn, et al., Combined iron chelator and T-type calcium channel blocker exerts greater efficacy on cardioprotection than monotherapy in iron-overload thalassemic mice, Eur. J. Pharmacol. 822 (2018) 43–50.
[17] D. Jamsai, F. Zaibak, W. Khongnium, J. Vadolas, L. Voullaire, K.J. Fowler, et al., A humanized mouse model for a common beta0-thalassemia mutation, Genomics 85 (2005) 453–461.
[18] D. Jamsai, F. Zaibak, J. Vadolas, L. Voullaire, K.J. Fowler, S. Gazeas, et al., A humanized BAC transgenic/knockout mouse model for HbE/beta-thalassemia, Genomics 88 (2006) 309–315.
[19] T. Incharoen, C. Thephinlap, S. Srichairatanakool, S. Chattipakorn, P. Winichagoon, S. Fucharoen, et al., Heart rate variability in beta-thalassemic mice, Int. J. Cardiol. 121 (2007) 203–204.
[20] S. Kumfu, S. Chattipakorn, K. Chinda, S. Fucharoen, N. Chattipakorn, T-type calcium channel blockade improves survival and cardiovascular function in thalassemic mice, Eur. J. Haematol. 88 (2012) 535–548.
[21] V. Berdoukas, K. Farmaki, S. Carson, J. Wood, T. Coates, Treating thalassemia major-related iron overload: the role of deferiprone, J. Blood Med. 3 (2012) 119–129.
[22] Y. MA, M. Podinovskaia, P.J. Evans, G. Emma, U.E. Schaible, J. Porter, et al., A novel method for non-transferrin-bound iron quantification by chelatable fluorescent beads based on flow cytometry, Biochem. J. 463 (2014) 351–362.
[23] B. Kulawiak, A.P. Kudin, A. Szewczyk, W.S. Kunz, BK channel openers inhibit ROS production of isolated rat brain mitochondria, Exp. Neurol. 212 (2008) 543–547.
[24] J. Sripetchwandee, J. Sanit, N. Chattipakorn, S.C. Chattipakorn, Mitochondrial calcium uniporter blocker effectively prevents brain mitochondrial dysfunction caused by iron overload, Life Sci. 92 (2013) 298–304.
[25] J.M. Walker, The bicinchoninic acid (BCA) assay for protein quantitation, Methods Mol. Biol. 32 (1994) 5–8.
[26] G. Beck, K. Shinzawa, H. Hayakawa, K. Baba, T. Yasuda, H. Sumi-Akamaru, et al., Deficiency of calcium-independent phospholipase A2 beta induces brain iron accumulation through upregulation of divalent metal transporter 1, PLoS One 10 (2015) e0141629.
[27] T. Skjorringe, A. Burkhart, K.B. Johnsen, T. Moos, Divalent metal transporter 1 (DMT1) in the brain: implications for a role in iron transport at the blood-brain barrier, and neuronal and glial pathology, Front. Mol. Neurosci. 8 (2015) 19.
[28] Y.Z. Chang, Y. Ke, J.R. Du, G.M. Halpern, K.P. Ho, L. Zhu, et al., Increased divalent metal transporter 1 expression might be associated with the neurotoxicity of L-DOPA, Mol. Pharmacol. 69 (2006) 968–974.
[29] M.O. Bostanci, F. Bagirici, Blocking of L-type calcium channels protects hippocampal and nigral neurons against iron neurotoxicity. The role of L-type calcium channels in iron-induced neurotoxicity, Int. J. Neurosci. 123 (2013) 876–882.
[30] J.A. Gaasch, W.J. Geldenhuys, P.R. Lockman, D.D. Allen, C.J. Van der Schyf, Voltage-gated calcium channels provide an alternate route for iron uptake in neuronal cell cultures, Neurochem. Res. 32 (2007) 1686–1693.
[31] J.A. Lockman, W.J. Geldenhuys, K.A. Bohn, S.F. Desilva, D.D. Allen, C.J. Van der Schyf, Differential effect of nimodipine in attenuating iron-induced toxicity in brain- and blood-brain barrier-associated cell types, Neurochem. Res. 37 (2012) 134–142.
[32] S. Kumfu, S. Chattipakorn, S. Srichairatanakool, J. Settakorn, S. Fucharoen, N. Chattipakorn, T-type calcium channel as a portal of iron uptake into cardiomyocytes of beta-thalassemic mice, Eur. J. Haematol. 86 (2011) 156–166.
[33] M.E. Lull, M.L. Block, Microglial activation and chronic neurodegeneration, Neurotherapeutics 7 (2010) 354–365.
[34] R.B. Rock, G. Gekker, S. Hu, W.S. Sheng, M. Cheeran, J.R. Lokensgard, et al., Role of microglia in central nervous system infections, Clin. Microbiol. Rev. 17 (2004) 942–964 (table of contents).
[35] G.W. Kreutzberg, Microglia: a sensor for pathological events in the CNS, Trends Neurosci. 19 (1996) 312–318.
[36] C.A. Colton, D.L. Gilbert, Production of superoxide anions by a CNS macrophage, the microglia, FEBS Lett. 223 (1987) 284–288.
[37] S.D. Hurley, S.A. Walter, S.L. Semple-Rowland, W.J. Streit, Cytokine transcripts expressed by microglia in vitro are not expressed by ameboid microglia of the developing rat central nervous system, Glia 25 (1999) 304–309.
[38] M.L. Block, L. Zecca, J.S. Hong, Microglia-mediated neurotoxicity: uncovering the molecular mechanisms, Nat. Rev. Neurosci. 8 (2007) 57–69.
[39] C.C. Chao, S. Hu, T.W. Molitor, E.G. Shaskan, P.K. Peterson, Activated microglia mediate neuronal cell injury via a nitric oxide mechanism, J. Immunol. 149 (1992) 2736–2741.
[40] E. Cekanaviciute, M. S. Buckwalter Astrocytes, Integrative regulators of neuroinflammation in stroke and other neurological diseases, Neurotherapeutics 13 (2016) 685–701.
[41] R.E. Gonzalez-Reyes, M.O. Nava-Mesa, K. Vargas-Sanchez, D. Ariza-Salamanca, L. Mora-Munoz, Involvement of astrocytes in alzheimer's disease from a neuroinflammatory and oxidative stress perspective, Front. Mol. Neurosci. 10 (2017) 427.
[42] S. Da Mesquita, A.C. Ferreira, J.C. Sousa, M. Correia-Neves, N. Sousa, F. Marques, Insights on the pathophysiology of Alzheimer's disease: the crosstalk between amyloid pathology, neuroinflammation and the peripheral immune system, Neurosci. Biobehav. Rev. 68 (2016) 547–562.
[43] C. Millington, S. Sonego, N. Karunaweera, A. Rangel, J.R. Aldrich-Wright, I.L. Campbell, et al., Chronic neuroinflammation in Alzheimer's disease: new perspectives on animal models and promising candidate drugs, BioMed Res. Int. 2014 (2014) 309129.
[44] K.S. Kirkley, K.A. Popichak, M.F. Afzali, M.E. Legare, R.B. Tjalkens, Microglia amplify inflammatory activation of astrocytes in manganese neurotoxicity, J. Neuroinflammation 14 (2017) 99.
[45] S.A. Liddelow, K.A. Guttenplan, L.E. Clarke, F.C. Bennett, C.J. Bohlen, L. Schirmer, et al., Neurotoxic reactive astrocytes are induced by activated microglia, Nature 541 (2017) 481–487.
[46] K. Saijo, B. Winner, C.T. Carson, J.G. Collier, L. Boyer, M.G. Rosenfeld, et al., A Nurr1/CoREST pathway in microglia and astrocytes protects dopaminergic neurons from inflammation-induced death, Cell 137 (2009) 47–59.
[47] F.X. Meng, J.M. Hou, T.S. Sun, In vivo evaluation of microglia activation by intracranial iron overload in central pain after spinal cord injury, J. Orthop. Surg. Res. 12 (2017) 75.
[48] O.M. Ogundele, A.O. Omoaghe, D.C. Ajonijebu, A.A. Ojo, T.D. Fabiyi, O.J. Olajide, et al., Glia activation and its role in oxidative stress, Metab. Brain Dis. 29 (2014) 483–493.
[49] H. Xu, Y. Wang, N. Song, J. Wang, H. Jiang, J. Xie, New progress on the role of glia in iron metabolism and iron-induced degeneration of dopamine neurons in Parkinson's disease, Front. Mol. Neurosci. 10 (2017) 455.
[50] L. Marschner, A. Schreurs, B. Lechat, J. Mogensen, A. Roebroek, T. Ahmed, et al., Single Mild Traumatic Brain Injury Results in Transiently Impaired Spatial Long-Term Memory and Altered Search Strategies, Behav Brain Res, 2018.
[51] E.A. Bordt, B.M. Polster, NADPH oxidase- and mitochondria-derived reactive oxygen species in proinflammatory microglial activation: a bipartisan affair? Free Radic. Biol. Med. 76 (2014) 34–46.
[52] T. Jiang, J. Hoekstra, X. Heng, W. Kang, J. Ding, J. Liu, et al., P2X7 receptor is critical in alpha-synuclein–mediated microglial NADPH oxidase activation, Neurobiol. Aging 36 (2015) 2304–2318.
[53] L. Qin, Y. Liu, J.S. Hong, F.T. Crews, NADPH oxidase and aging drive microglial activation, oxidative stress, and dopaminergic neurodegeneration following systemic LPS administration, Glia 61 (2013) 855–868.
[54] B.I. Giasson, H. Ischiropoulos, V.M. Lee, J.Q. Trojanowski, The relationship between oxidative/nitrative stress and pathological inclusions in Alzheimer's and Parkinson's diseases, Free Radic. Biol. Med. 32 (2002) 1264–1275.
[55] C.Y. Lee, G.E. Landreth, The role of microglia in amyloid clearance from the AD brain, J. Neural Transm. 117 (2010) 949–960.
[56] E. Solito, M. Sastre, Microglia function in Alzheimer's disease, Front. Pharmacol. 3 (2012) 14.
[57] A.Y. Abramov, L. Canevari, M.R. Duchen, Beta-amyloid peptides induce mitochondrial dysfunction and oxidative stress in astrocytes and death of neurons through activation of NADPH oxidase, J. Neurosci. 24 (2004) 565–575.
[58] D.Y. Liu, Z.D. Liu, R.C. Hider, Oral iron chelators–development and application, Best Pract. Res. Clin. Haematol. 15 (2002) 369–384.
[59] H. Tanaka, K. Shigenobu, Efonidipine hydrochloride: a dual blocker of L- and T-type ca(2+) channels, Cardiovasc. Drug Rev. 20 (2002) 81–92.
[60] C. Shudo, Y. Masuda, H. Sugita, S. Tanaka, K. Tomita, Effects of efonidipine hydrochloride (NZ-105), a new calcium antagonist, against acute renal failure in rats, Gen. Pharmacol. 25 (1994) 1451–1458.